

NUMERICAL MODELS FOR COSMIC RAY PROPAGATION AND GAMMA RAY PRODUCTION

A.W. Strong*, I.V. Moskalenko*[†], and V. Schönfelder*

**Max-Planck-Institut für extraterrestrische Physik, Postfach 1603, D-85740 Garching, Germany*

[†]*Institute for Nuclear Physics, M.V. Lomonosov Moscow State University, 119 899 Moscow, Russia*

ABSTRACT

An extensive program for the calculation of galactic cosmic-ray propagation has been developed. Primary and secondary nucleons, primary and secondary electrons, and secondary positrons are included. The basic spatial propagation mechanisms are (momentum-dependent) diffusion, convection, while in momentum space energy loss and diffusive reacceleration are treated. Fragmentation and energy losses are computed using realistic distributions for the interstellar gas and radiation fields.

INTRODUCTION

The main motivation for developing this code (Strong and Moskalenko 1997) is the prediction of diffuse Galactic gamma rays for comparison with data from the CGRO instruments EGRET, COMPTEL and OSSE. This is a development of the work described in Strong and Youssefi (1995). More generally the idea is to develop a model which self-consistently reproduces observational data of many kinds related to cosmic-ray origin and propagation: direct measurements of nuclei, electrons and positrons, gamma rays, and synchrotron radiation. These data provide many independent constraints on any model and our approach is able to take advantage of this since it must be consistent with all types of observation. We emphasize also the use of realistic astrophysical input (e.g. for the gas distribution) as well as theoretical developments (e.g. reacceleration). The code is sufficiently general that new physical effects can be introduced as required. The basic procedure is first to obtain a set of propagation parameters which reproduce the cosmic ray B/C ratio, and the spectrum of secondary positrons; the same propagation conditions are then applied to primary electrons. Gamma-ray and synchrotron emission are then evaluated. Models both with and without reacceleration are considered.

DESCRIPTION OF THE MODEL

The models are three dimensional with cylindrical symmetry in the Galaxy, the basic coordinates being (R, z, p) where R is Galactocentric radius, z is the distance from the Galactic plane and p is the total particle momentum. The numerical solution of the transport equation is based on a Crank-Nicholson implicit second-order scheme. In the models the propagation region is bounded by $z = z_h$ beyond which free escape is assumed. A value $z_h = 3$ kpc has been adopted since this is within the range which is consistent with studies of $^{10}\text{Be}/\text{Be}$ and synchrotron radiation. For a given z_h the diffusion coefficient as a function of momentum is determined by B/C for the case of no reacceleration; with reacceleration on the other hand it is the reacceleration strength (related to the Alfvén speed v_A) which is determined by B/C . Reacceleration provides a natural mechanism to reproduce the B/C ratio without an ad-hoc form for the diffusion coefficient (e.g., Heinbach and Simon 1995, Seo and Ptuskin 1994). The spatial diffusion coefficient for the case *without* reacceleration is $D = \beta D_0$ below rigidity ρ_0 , $\beta D_0 (\rho/\rho_0)^\delta$ above rigidity ρ_0 , where β is the particle speed. The spatial diffusion coefficient *with* reacceleration assumes a Kolmogorov spectrum of weak MHD turbulence so $D = \beta D_0 (\rho/\rho_0)^\delta$ with $\delta = 1/3$ for all rigidities. For this case the momentum-space diffusion coefficient is related to the spatial coefficient (Seo and Ptuskin 1994). The injection spectrum of nucleons is assumed to be a power law in momentum for the different species, $dq(p)/dp \propto p^{-\gamma}$ for the injected *density*, corresponding to an injected *flux* $dF(E_k)/dE_k \propto p^{-\gamma}$ where E_k is the kinetic energy per nucleon.

The entire calculation is performed with momentum as the kinematic variable. The interstellar

fraction of the gas is taken as 0.11 by number. The interstellar radiation field for inverse Compton losses is based on stellar population models and IRAS and COBE data, plus the cosmic microwave background. The magnetic field is assumed to have the form $6e^{-(|z|/5\text{kpc})-(R/20\text{kpc})} \mu\text{G}$. Energy losses for electrons by ionization, Coulomb, bremsstrahlung, inverse Compton and synchrotron are included, and for nucleons by ionization and Coulomb interactions. The distribution of cosmic-ray sources is chosen to reproduce the cosmic-ray distribution determined by analysis of EGRET gamma-ray data (Strong and Mattox 1996). The bremsstrahlung and inverse Compton gamma rays are computed self-consistently from the gas and radiation fields used for the propagation. The π^0 -decay gamma rays are calculated directly from the proton and Helium spectra using the method of Dermer (1986). The secondary nucleon and secondary e^\pm source functions are computed from the propagated primary distribution and the gas distribution, and the anisotropic distribution of e^\pm in the μ^\pm system was taken into account.

ILLUSTRATIVE RESULTS

Some results obtained are shown in the Figures.

Fig. 1: Secondary nucleons. The energy dependence of the B/C ratio can be reproduced with $D_0 = 2.0 \times 10^{28} \text{ cm}^2 \text{ s}^{-1}$, $\delta = 0.6$, $\rho_0 = 3 \text{ GV/c}$ without reacceleration (thick line) and $D_0 = 4.2 \times 10^{28} \text{ cm}^2 \text{ s}^{-1}$, $v_A = 20 \text{ km s}^{-1}$ with reacceleration (thin line). Dashed lines are modulated to 500 MV. Data from Webber et al. (1996).

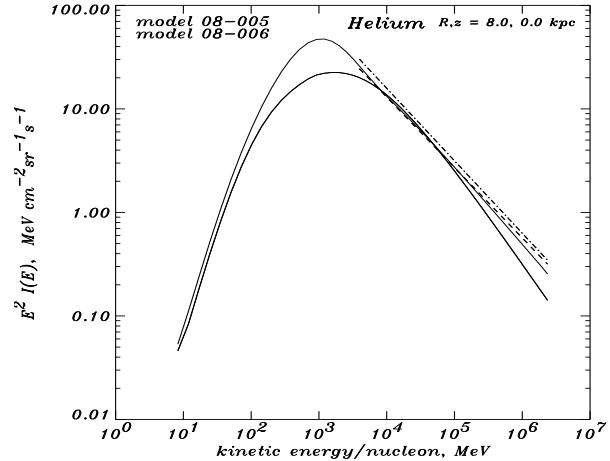
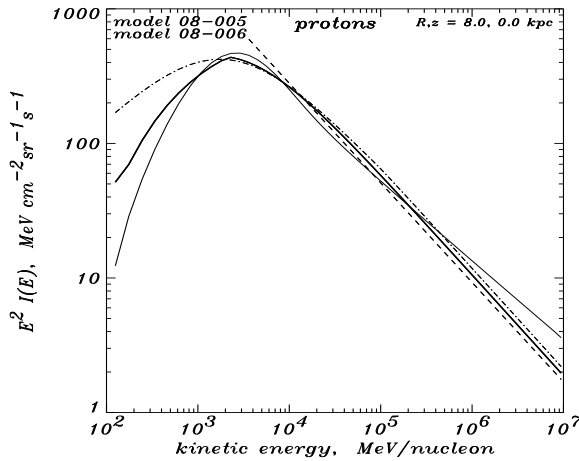
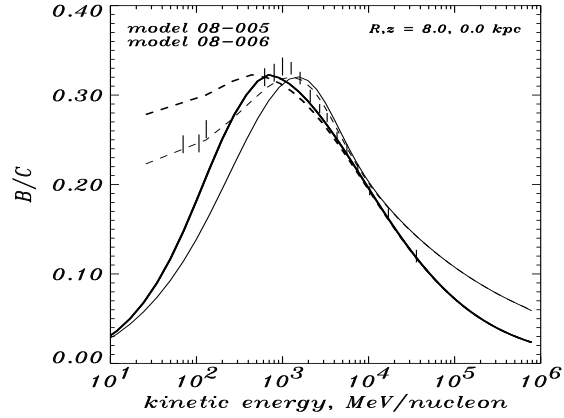


Fig. 2: Left panel: the local proton spectrum for injection index 2.15 (thin solid line), 2.25 (thick solid line) without and with reacceleration respectively, compared with the measured ‘interstellar’ spectrum (dashed line: Seo et al. 1991, dashed-dot line: Mori 1997). *Right panel:* the Helium spectrum with injection index 2.25 (thin solid line), 2.45 (thick solid line) without and with reacceleration respectively, compared with the measured ‘interstellar’ spectrum (dashed line: Seo et al. 1991, dashed-dot line: Engelmann et al. 1990). The spectra are well reproduced up to 100 GeV.

Secondary positrons and electrons: Using the primary proton and Helium spectra, the propagation of secondary e^\pm has been computed. The e^+ spectrum (Fig 3) and the positron fraction (Fig 4) agrees well with the most recent data compilation for 0.1–10 GeV; for more details see Moskalenko and Strong (1997).

Primary electrons: The spectrum of primary electrons is also shown in Fig 3. The adopted electron injection spectrum has a power law index -2.1 up to 10 GeV; this is chosen using the constraints

around 10 GeV where solar modulation is small and it also satisfies the constraints from $\frac{e^+}{e^+ + e^-}$. Above 10 GeV a break is required to at least -2.4 for agreement with direct measurements (which may however not be necessary if local sources dominate the directly measured high-energy electron spectrum).

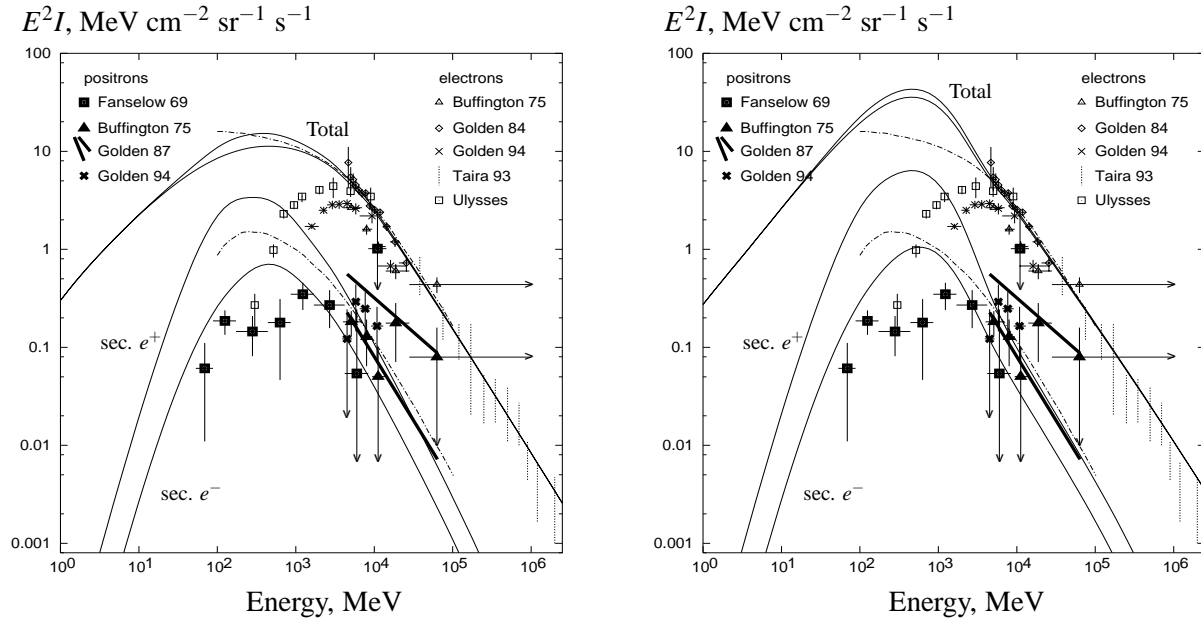


Fig. 3: Spectra of secondary positrons and electrons, and of primary electrons. Full lines: our model with no reacceleration (left panel) and with reacceleration (right panel). Dash-dotted lines (Protheroe 1982): lower is his leaky-box prediction for e^+ , upper is his electron spectrum.

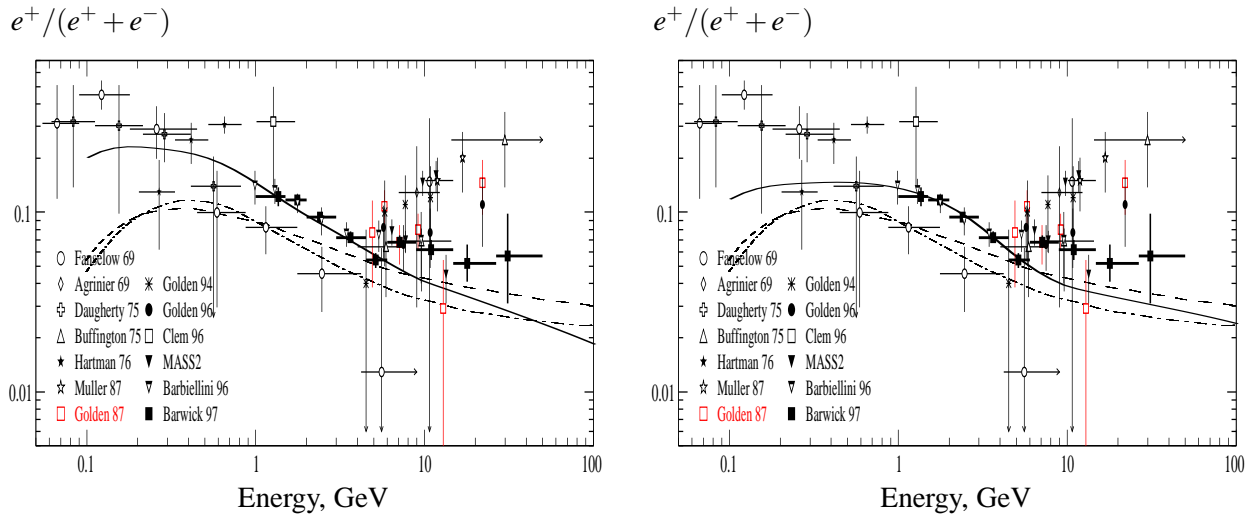


Fig. 4: Positron fraction for model with no reacceleration (left panel) and with reacceleration (right panel). Dashed and dash-dotted lines: Protheroe (1982) predictions of the leaky-box and diffusive halo models respectively. The data collection is taken from Barwick et al. (1997).

The synchrotron spectrum (Fig 5) at high Galactic latitudes is important since its shape constrains the shape of the 1–10 GeV electron spectrum. An injection index -2.1 (without reacceleration) is the steepest which is allowed by the radio data over the range 38 to 1420 MHz. As illustrated, an index -2.4 as often used (e.g. Strong et al. 1996) gives a synchrotron spectrum which is too steep.

The modelled gamma-ray spectrum for the inner Galaxy, illustrated here for the case of no reacceleration (Fig 6), fits well the COMPTEL and EGRET data up to 500 MeV beyond which there is the well-known excess not accounted for by π^0 -decay with the standard nucleon spectrum. The

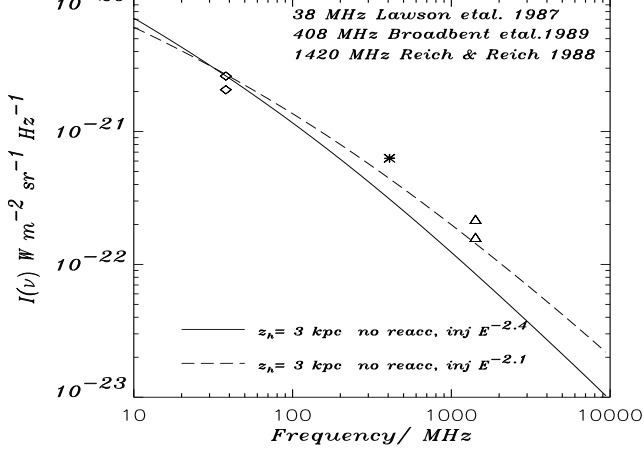


Fig. 5: The synchrotron spectrum at the NGP, compared to predictions for electron injection indices -2.1 (dashed line) and -2.4 (solid line).

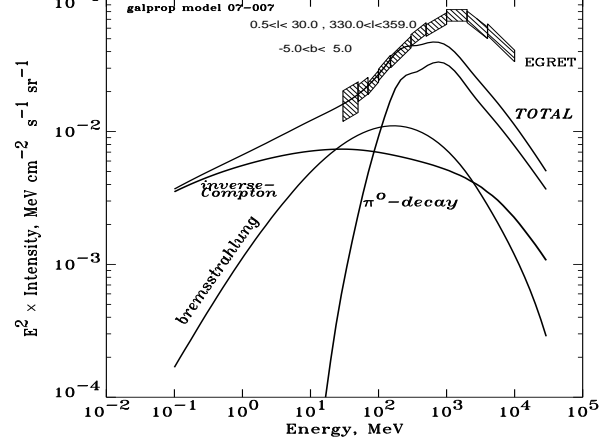


Fig. 6: The γ -ray spectrum for the inner Galaxy, $330^\circ < l < 30^\circ$, $|b| < 5^\circ$. EGRET data: Strong and Mattox (1996).

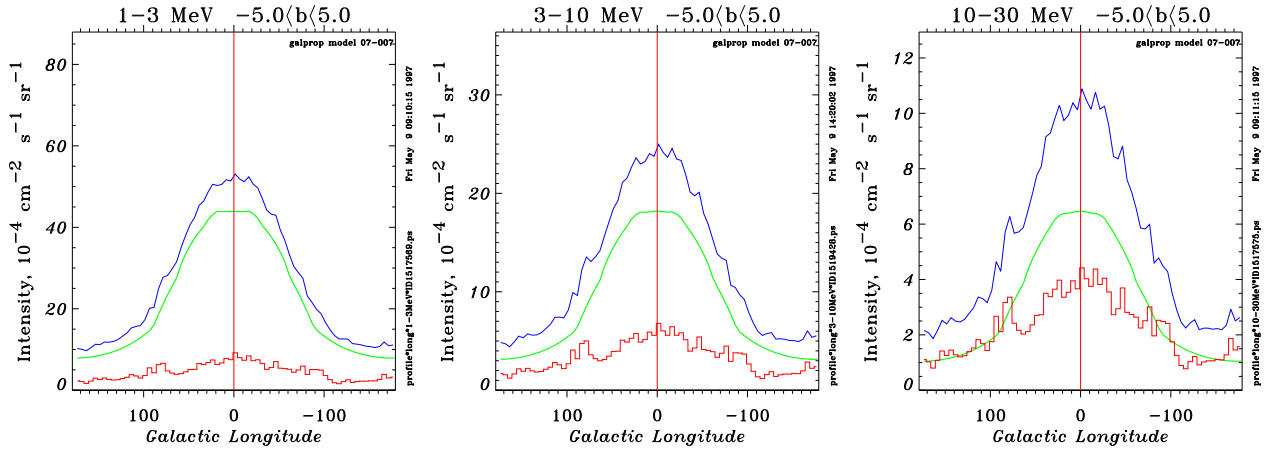


Fig. 7: The model γ -ray longitude profile ($|b| < 5^\circ$) for bremsstrahlung (histogram), inverse Compton (middle curve) and total (upper curve), for energies 1–3, 3–10 and 10–30 MeV.

COMPTEL spectrum from a recent analysis by Strong et al. (1997) is both lower and flatter than previously published. It fits well to the flatter electron injection spectrum required by synchrotron data (see above). Inverse Compton is dominant below 10 MeV, bremsstrahlung becomes important for 3–200 MeV. The lower bremsstrahlung combined with π^0 -decay leads to a good fit to the steep rise in this range, in contrast to previous attempts to model the spectrum with a steeper bremsstrahlung spectrum (Strong et al. 1996). Below 10 MeV inverse Compton becomes increasingly dominant, and bremsstrahlung is negligible below 1 MeV. The longitude profile (Fig 7) at low latitudes from this model is compared with that from COMPTEL elsewhere (Strong et al. 1997). The large energy dependence of the relative importance of inverse Compton and bremsstrahlung is evident.

More details can be found on <http://www.gamma.mpe-garching.mpg.de/~aws/aws.html>

REFERENCES

- | | |
|---|--|
| Barwick S.W. et al., ApJL, 482, L191 (1997) | Strong A.W., and Mattox J.R., A&A, 308, L21 (1996) |
| Dermer C.D., A&A, 157, 223 (1986) | Strong A.W., and Moskalenko I.V., Proc. 4th Compton Symp., AIP (1997) |
| Engelmann J.J. et al., A&A, 233, 96 (1990) | Strong A.W., and Youssefi G., Proc. 24th ICRC 3, 48 (1995) |
| Heinbach U., and Simon M., ApJ, 441, 209 (1995) | Strong A.W. et al., Proc. 3rd Compton Symp., A&A Supp 120, C381 (1996) |
| Mori M., ApJ, 478, 225 (1997) | Strong A.W. et al., Proc. 4th Compton Symp., AIP (1997) |
| Moskalenko I.V., and Strong A.W., in preparation (1997) | Webber W.R. et al., ApJ, 457, 435 (1996) |
| Protheroe R.J., ApJ, 254, 391 (1982) | |
| Seo E.S., and Ptuskin V.S., ApJ, 431, 705 (1994) | |
| Seo E.S. et al., ApJ, 378, 763 (1991) | |